

Thermoelectric effect in nano-scaled lanthanides doped ZnO

Otal E. H.¹, Schaeuble N.², Aguirre M. H.², Canepa H.R.¹, Walsöe de Reca N. E.¹

1 _ Centro de Investigación en Sólidos, CITEFA, San Juan Bautista de La Salle 4397 (B1603ALO) Villa Martelli, Buenos Aires, Argentina

2 _ Solid State Chemistry and Catalysis, Empa, Swiss Federal Laboratories for Materials Testing and Research, Ueberlandstrasse 129, CH-8600 Dübendorf, Switzerland

canepa@citefa.gov.ar

myriam.aguirre@empa.ch

Abstract. Start Nano-scaled ZnO with 1% Er doping was prepared by soft chemistry methods. The synthesis was carried out in anhydrous polar solvent to achieve a crystal size of a few nanometers. Resulting particles were processed as precipitates or multi layer films. Structural characterization was evaluated by X-Ray diffraction and transmission and scanning electron microscopy . In the case of films, UV-Vis characterization was made. The thermoelectrical properties of ZnO:Er were evaluated and compared with a typical good thermoelectric material ZnO:Al. Both materials have also shown high Seebeck coefficients and they can be considered as potential compounds for thermoelectric conversion.

1. Introduction

The ZnO is a common conductive oxide with a wide band gap of 3.5 eV. The electrical properties of ZnO are exploited in gas sensors [1] and varistors [2, 3]. Furthermore, materials derived from ZnO have been investigated as potential candidates for high-performance n-type oxide thermoelectric materials. The thermoelectric properties of undoped and doped ZnO (e.g. ZnO:Al, ZnO:Sb, ZnO:Pr) are well studied [4-13]. The best thermoelectric properties were obtained with Al-doped ZnO by Ohtaki and Tsubota et al. [4,7]. Fujishiro et al. reported the effect of microstructural control on thermoelectric properties of hot-pressed Al-doped ZnO [14]. After hot pressing, dense products of polycrystalline $Zn_{0.99}Al_{0.01}O$, containing nanosized grains with sizes below 1 μm in diameter were obtained. The power factor $S^2\sigma$ of the nanostructured $Zn_{0.99}Al_{0.01}O$ prepared by hot pressing was higher in the measured temperature range (300°C to 800 °C) than that of polycrystalline $Zn_{0.99}Al_{0.01}O$ prepared by normal sintering at 1400 °C. Enhanced thermoelectric performance of nanostructured ZnO were also reported by Ohtaki et al. [15]. Highly dispersed nanosized closed pores (nanovoids) are revealed to be effective to substantially enhance the thermoelectric performance of bulk sintered body of n-type Al-doped ZnO, resulting in a dimensionless figure-of-merit of $ZT = 0.65$ at 1250 K. Rare earths cations are interesting because of their large ionic radii and trivalent oxidation state. Metals of the d-group are usually introduced into ZnO matrix, occupying substitution or interstitial site. Due to

its mayor ionic radii, lanthanides are not easily introduced and phase segregation is produced [16]. The route reported by Schwartz [17] uses polar aprotic solvents to solvate cations in solution and obtain nanostructured ZnO. The results of its modification to obtain erbium doped ZnO are shown below.

1. Experimental

The Erbium-doped samples were prepared by soft chemistry process: Zinc acetate dihydrate and Erbium acetate hydrate were dissolved in dimethylformamide and basified by drop wise of a KOH ethanolic solution under vigorous agitation. Once the base was aggregated, the colloids were precipitated by ethyl acetate and centrifuged to separate the solid from the supernatant. To eliminate residues of solvent, particles were suspended in ethanol, precipitated twice in ethyl acetate and dried in vacuum.

Films were prepared by spin coating from the final solution and dried at 800K for 5 minutes. Multilayer films were obtained by this proceeding. For optical characterization, fused quartz (GM associates Inc) was used as substrate and for microscopy characterization silicon wafers were used.

XRD was measured from dried samples. A PW 3710 Philips diffractometer was used to do these measurements. Instrumental broadening was corrected by LaB₆ standard. Samples and standard were measured in Bragg Brentano configuration in the range 10°-100° with 0.02°/step.

For TEM analysis, powder samples suspended in alcohol were deposited in holey carbon copper grid. SEM images were obtained from films deposited over Silicon. The TEM and SEM analysis were performed in a Philips CM30 at 300 kV and a Karl Zeiss FESEM DSM 982 GEMINI, respectively.

Spectrometric measurements were performed in a multi-wavelength diode array HP 8453 spectrophotometer (Hewlett Packard, Palo Alto, CA, USA) controlled through the Chem-Station software package. Samples were measured perpendicular to incident light in a modified sample holder. Quartz substrate without ZnO film was used as blank.

Electrical conductivity and Seebeck coefficient were measured simultaneously in the temperature range of $330\text{ K} \leq T \leq 1273\text{ K}$, in pressed powder pellets prepared by sintering at 1272 K for 1h. The electrical resistivity ρ was measured by the DC four-probe technique by Ozawa Science equipment: two platinum contacts placed at the ends of the bar-shaped sample supply the current and two platinum wires looped around the pellet measure the potential difference. The Seebeck coefficient was measured in the following way: a well defined temperature gradient was applied to the sample by cooling one end with cold air and the voltage difference generated by the sample was recorded. The temperature gradient was measured by two thermocouples (Pt / Pt + 13 % Rh) attached to the platinum layer contacts. The Seebeck coefficient of the sample was finally obtained after extracting the contribution of the thermocouple ($S_{\text{sample}} = S_{\text{measured}} - S_{\text{Pt}}$).

2. Results and discussion

The XRD of solids showed a broadening due to the particle size (figure 1). The peak broadening showed a small anisotropy in the a-axis direction. The average particle size over the first peaks, corrected by instrumental broadening, was 10nm. This size is bigger than Bohr radius for ZnO [18] and in consequence nanoscale constituents would not introduce quantum-confinement effects to enhance the power factor $S^2\sigma$.

Samples showed a uniform growth and thickness was increased by increasing the number of deposited layers. This was confirmed by UV-Vis spectroscopy. The absorbance of the films deposited on fused quartz exhibited a linear correlation with number of layers, indicating a linear increase of deposited mass. An approximate thickness of 60nm/layer was obtained.

Films conserved the same nanostructure after deposited and dried, as can be observed in SEM image in figure 2. Most of particles remain in the nanometric size after depositing while a few needlesgrothw over the surface but keeping the nano-scale range

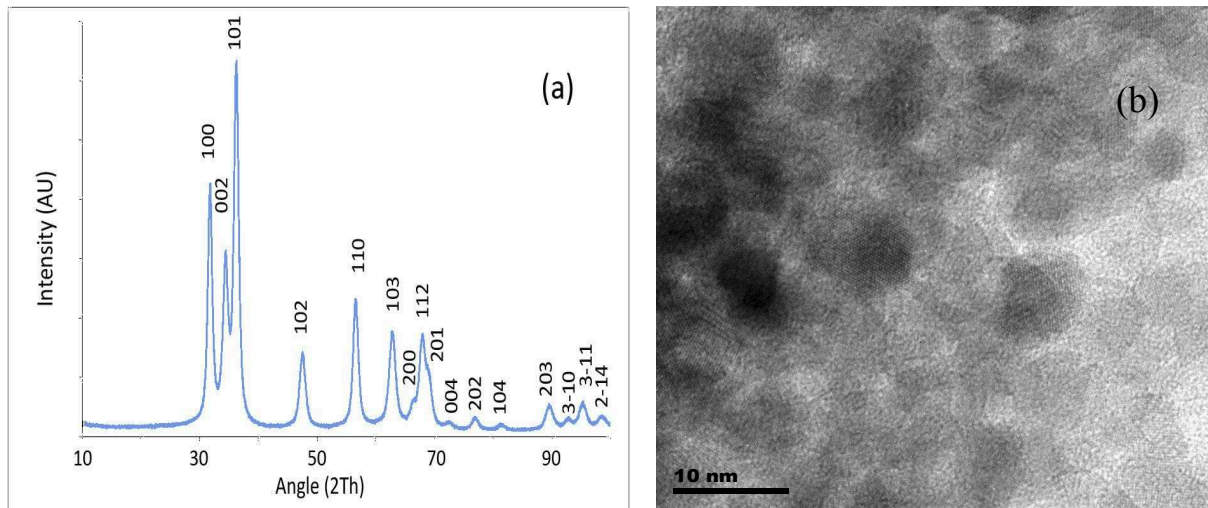


Fig 1 – a) XRD pattern diffraction for erbium doped ZnO sample. b) HRTEM micrographs for erbium doped ZnO before precipitated. The peak broadening due to the nanosized crystals was confirmed by TEM.

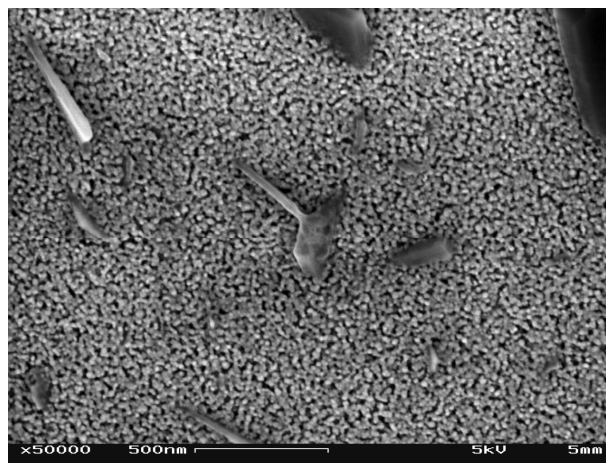


Figure 2 - Scanning microscopy of the planar view of a film.

The Seebeck coefficient and electrical conductivity were summarized as a function of temperature in figure 3 (a) and (b) , respectively. The Seebeck coefficient measurements for ZnO:Er showed a value of -510mW/K , while ZnO:Al is reported to be -550 mW/K [19] . This values shows a p-type behavior of ZnO:Er and comparable thermoelectric properties with ZnO:Al. The conductivity of the sample shows a resistance of 4kΩ.cm at 475K and 1Ω.cm at 1200K. A transition from insulator to semiconductor is observed. This abrupt change can be attributed to modifications in electronic

level population produced by changing in erbium location sites, although many others phenomena could contribute to this like oxygen loss, zinc valence change and crystal cell parameters reduction. Studies of photoluminescence, XAS (XANES, EXAFS and XEOL) and XRD, of samples calcinated at different temperatures, are being performed which will help to obtain more information about this process. Preliminary results exhibited changes in luminescence spectra, showing a transition from a disordered site to a more crystalline and symmetric one, which seems to support our supposition.

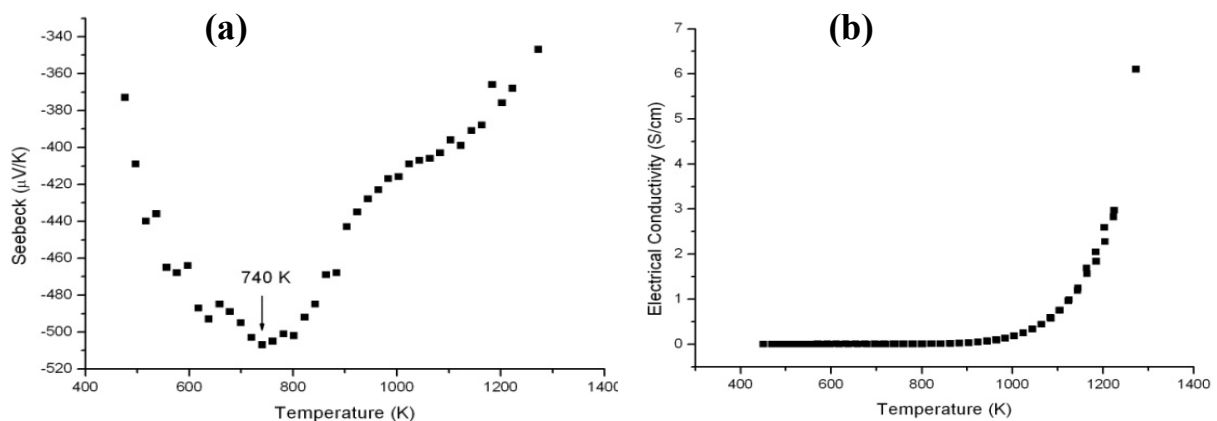


Figure 3 – a) Temperature dependence of Seebeck coefficient. At 740K a minimum is observed, b) Temperature dependence of electrical conductivity.

3. Conclusions

Efficient erbium introduction into ZnO was achieved by wet chemistry methods.

High Seebeck coefficient was obtained for ZnO:Er. This value was compared with Seebeck coefficient of typical good thermoelectric material.

An abrupt change in electrical conductivity was found at 790K, probably related to changes in erbium environment with temperature. Studies of photoluminescence, XAS (XANES, EXAFS and XEOL) and XRD of samples calcinated at different temperatures are being performed in order to obtain more information about this process

Acknowledgments

The authors are indebted to YPF Foundation, CITEFA, CONICET and EMPA for financial support that enabled them to accomplish this work.

References

- [1] S.-N. Bai, T.-Y. Tseng, *Journal of Applied Physics* 74 (1), pp. 695-703 (1993).
- [2] Bok-Hee Lee, Sung-Man Kang, *Current Applied Physics* (6), 5, pp 844-851 (2006).
- [3] Y.-M. Chiang, W.D. Kingery, L.M. Levinson, *Journal of Applied Physics* 53 (3), pp. 1765-1768 (1982).
- [4] Tsubota, T., Ohtaki, M., Eguchi, K., Arai, H., *J. Mater. Chem.* 7 (1), 85 - 90 (1997).

- [5] Tsubota, T., Ohtaki, M., Eguchi, K., Arai, H., International Conference on Thermoelectrics, ICT, Proceedings, pp. 240-243 (1997).
- [6] Ohtaki, M., Tsubota, T., Eguchi, K., Arai, H., Journal of Applied Physics 79 (3), pp. 1816-1818, (1996).
- [7] Ohtaki, Michitaka, Tsubota, Toshiki, Eguchi, Koichi, International Conference on Thermoelectrics, ICT, Proceedings, pp. 610-613 (1998).
- [8] K. Park, J.K. Seong, S. Nahm, J. of Alloys and Compounds, 455 (1-2), 331-335 (2008).
- [9] Tanaka Y., Ifuku T., Tsuchida K., Kato A., Journal of Material Science Letters 16, 155 - 157 (1997).
- [10] Kaga, H., Kinemuchi, Y., Tanaka, S., Makiya, A., Kato, Z., Uematsu, K., Watari, K., Japanese Journal of Applied Physics, Part 2: Letters, Volume 45, Issue 42-45, 10 November 2006, Pages L1212-L1214.
- [11] Inoue, Y., Okamoto, Y., Morimoto, J., Journal of Materials Science, Volume 43, Issue 1, Pages 368-377 (2008).
- [12] Inoue, Y., Okamoto, M., Kawahara, T., Okamoto, Y., Morimoto, J. Materials Transactions, Volume 46, Issue 7, Pages 1470-1475 (2005).
- [13] Fuda, K., Sugiyama, S., Materials Research Society Symposium Proceedings Volume 886, Pages 473-478 (2006).
- [14] Fujishiro Y., Miyata, M., Awano, M., Maeda, K., J. Am. Ceram. Soc. 86 (12) 2063 - 2066 (2003).
- [15] Ohtaki, M., Hayashi, R., International Conference on Thermoelectrics, ICT, Proceedings, art. no. 4133287, pp. 276-279 (2006).
- [16] Mustafa D., Biggemann D., Wu J., Coffey J. L. and Tessler L.R., Superlattices and Microstructures Volume 42, Issues 1-6, July-December 2007, Pages 403-408
- [17] Schwartz, D. A.; Norberg, N. S.; Nguyen, Q. P.; Parker, J. M.; Gamelin, D. R., Journal of the American Chemical Society ; 2003; 125(43); 13205-13218
- [18] Brus L.E. Journal of Physical Chemistry. 1986, 90, 2555-2560
- [19] Schäuble N. – Diploma Thesis. EMPA – Zurich, Switzerland – July 2008